

University of São Paulo
São Carlos School of engineering



Sistemas de Controle

List 4

Professor: Adriano Siqueira

Student: Jhon Charaja

São Carlos - Brasil

2021 - 2

1 Question 1

Considering the transfer function (G)

$$G = \frac{w_n^2}{s^2 + 2w_n\zeta s + w_n^2},$$

where ζ is damping factor and w_n is natural frequency.

The modulus of G at resonance frequency (w_r) is given by

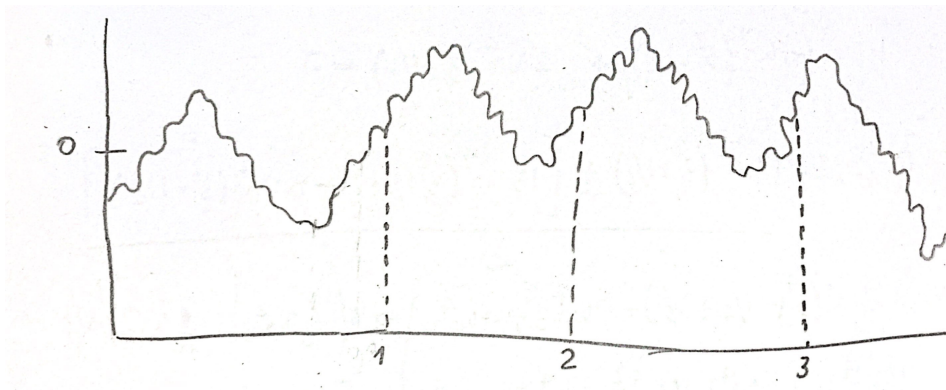
$$|G(jw_r)| = \frac{w_n^2}{\sqrt{(w_n^2 - w_r^2)^2 + (2w_n\zeta w_r)^2}} = \frac{1}{2\zeta\sqrt{1 - \zeta^2}},$$

Then resonance frequency can be computed in function of w_n and ζ as

$$\begin{aligned} 0 &= w_n^4 + w_r^2(-2w_n^2 + 4w_n^2\zeta^2) + w_n^4(1 - 4\zeta^2(1 - \zeta^2)) \\ w_r^2 &= w_n^2 - 2w_n^2\zeta^2, \\ w_r &= w_n\sqrt{1 - 2\zeta^2} \end{aligned}$$

2 Question 2

(a) The bode diagram indicates that close-loop system attenuates signals with frequency higher than 4.5 Hz and delay output signal with respect to input. Thus, response of close-loop system will present lower oscillations. Figure 1 describes a sketch of response of close-loop system.



Scanned with CamScanner

Figure 1: Sketch of response of close-loop system.

(b) Considering input signal

$$r(t) = 1 \sin(2\pi 0.1t) + 0.5 \sin(2\pi t) + 0.2 \sin(2\pi 10t),$$

the output signal will be

$$y(t) = 1 \sin(0.628t + 0 \text{ rad}) + 0.48 \sin(6.28t - 0.262 \text{ rad}) + 0.0796 \sin(62.8t - 1.08 \text{ rad}),$$

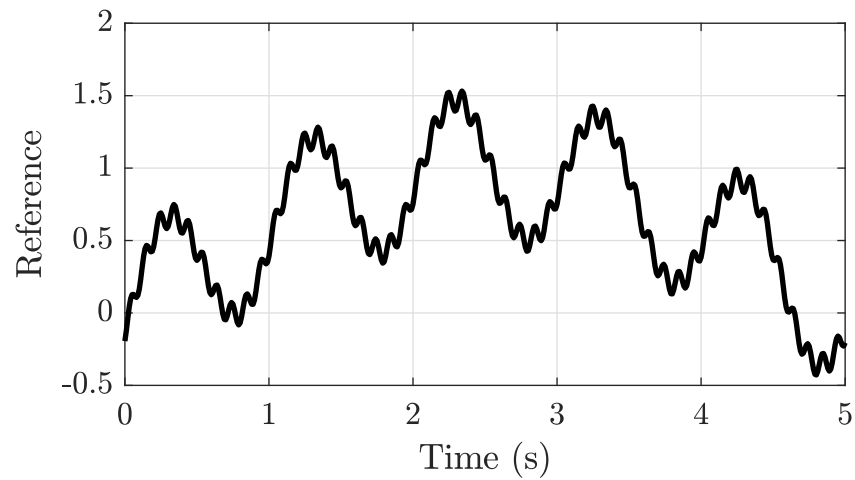


Figure 2: Response of the close-loop system with input (2).

3 Question 3

(a) Dynamic model is given by

$$\begin{aligned} I_1 \ddot{\theta}_1 &= \tau - K(\theta_1 - \theta_2) - D(\dot{\theta}_1 - \dot{\theta}_2), \\ I_2 \ddot{\theta}_2 &= K(\theta_1 - \theta_2) + D(\dot{\theta}_1 - \dot{\theta}_2), \end{aligned}$$

where K is stiffness and D is damping.

(b) Transfer functions are:

$$\begin{aligned} G_1(s) &= \frac{\theta_1(s)}{\tau(s)} = \frac{I_2 s^2 + Ds + k}{I_1 I_2 s^4 + s^3(I_1 D + I_2 D) + s^2(I_1 K + I_2 K)}, \\ G_2(s) &= \frac{\theta_2(s)}{\tau(s)} = \frac{Ds + k}{I_1 I_2 s^4 + s^3(I_1 D + I_2 D) + s^2(I_1 K + I_2 K)}. \end{aligned}$$

(c) Figure 3 describes time-response of open-loop systems ($G_1(s)$ and $G_2(s)$) for different values of stiffness ($K = 10[1, 1.4, 1.8, 2.2, 2.6, 3] \frac{\text{N.m}}{\text{rad}}$) and damping ($D = 1000[1, 1.8, 2.6, 3.4, 4.2, 5] \frac{\text{N.m.s}}{\text{rad}}$).

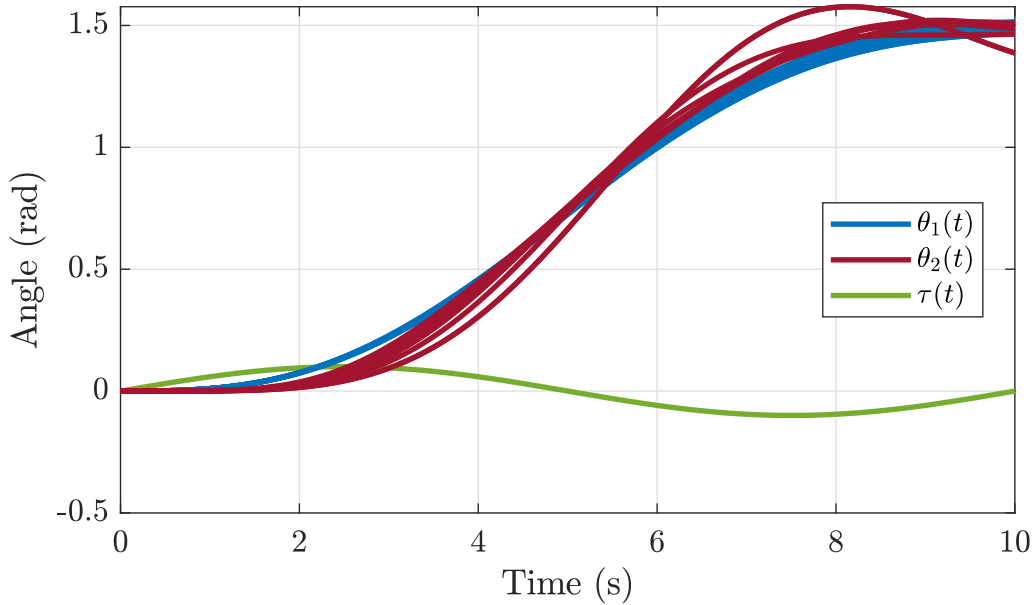


Figure 3: Time-response of open-loop systems ($G_1(s)$ and $G_2(s)$) considering sinusoidal input ($\tau = 0.1 \sin 0.2\pi t$) and different values of stiffness and damping ($K = 10[1, 1.4, 1.8, 2.2, 2.6, 3] \frac{\text{N.m}}{\text{rad}}$ and $D = 1000[1, 1.8, 2.6, 3.4, 4.2, 5] \frac{\text{N.m.s}}{\text{rad}}$).

(d) On one hand, Figure 4 describes root-locus of close-loop system with proportional gain. In this figure, third and fourth poles (p_3, p_4) are located in the right half-plane for any proportional gain value. On the other hand, Figure 5 describes

bode diagram of open-loop system ($G_2(s)$). In this figure, gain margin is $G_m = -13$ dB and phase margin is $P_m = 179^\circ$. Likewise, phase diagram is below -180° , thus gain margin will be negative for any proportional gain value. In conclusion, both root-locus and frequency response method indicates that close-loop system cannot be controlled with just a proportional gain.

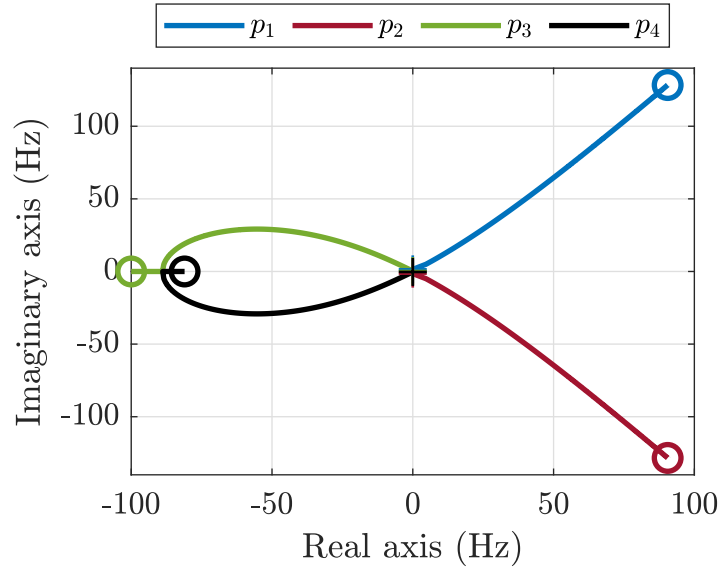


Figure 4: Root-Locus of close-loop system with proportional gain.

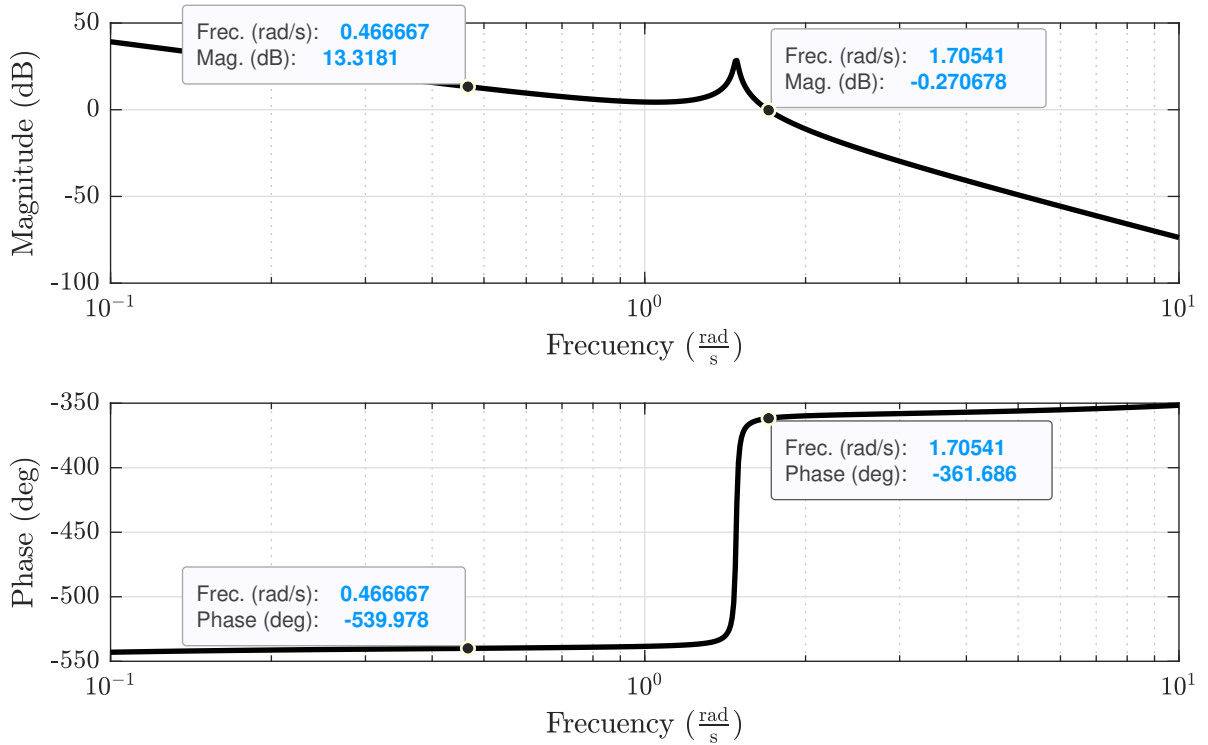


Figure 5: Frequency response of open-loop system $G_2(s) = \frac{\theta_2(s)}{\tau(s)}$.

(e) On one hand, Figure 6 describes root-locus of close-loop system with proportional-derivative gain. In this figure, poles are located in the left half-plane for proportional gain from 0.0001 to 0.275 and derivative gain from 0.00001 to 0.0275; then, first and second poles (p_1, p_2) move to right half-plane and close-loop system becomes unstable. On the other hand, Figure 7 describes bode diagram of close-loop system with proportional-derivative control method. In this figure, gain margin is greater than 0 dB for proportional and derivative gains lower than 0.275 and 0.0275, respectively. Likewise, resonance peak is above 0 dB when gain margin is lower than 0 dB.

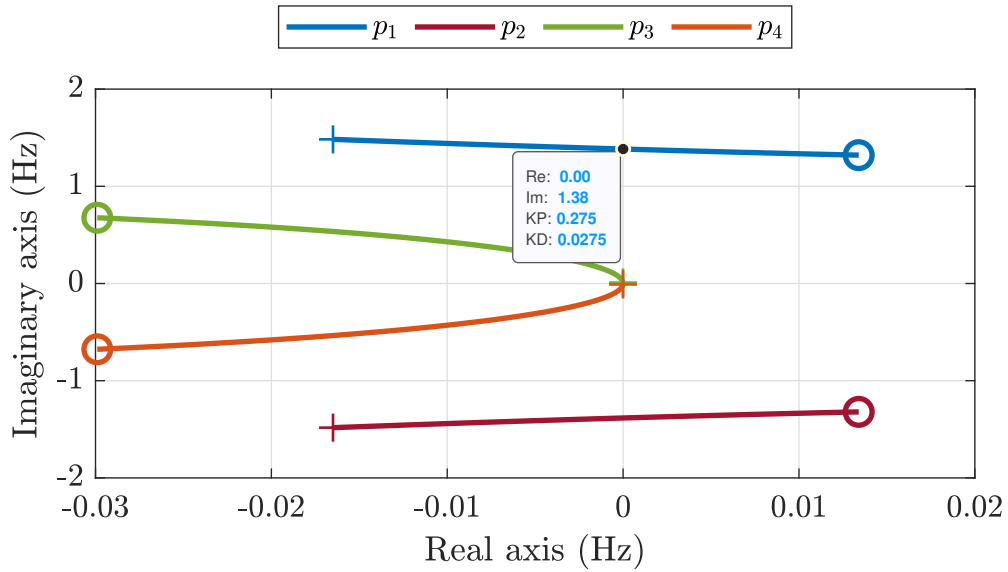


Figure 6: Closed-loop system pole location diagram with proportional-derivative control method. Likewise, information box indicates maximum proportional and derivative gains until system becomes unstable.

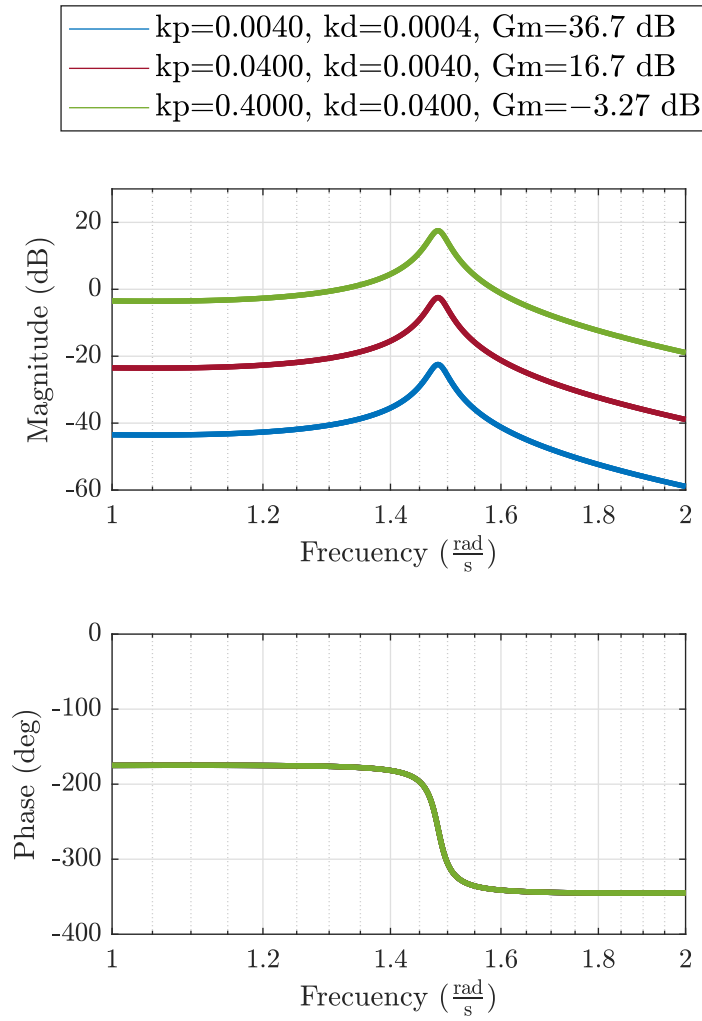


Figure 7: Frequency response of open-loop system $G_2(s) = \frac{\theta_2(s)}{\tau(s)}$.

(f) Figure 6 indicates that close-loop system have imaginary poles two times. On one hand, at the beginning ($k_p = 0.0001$ and $k_d = 0.0001$), third and fourth poles are $+0.0095i$ and $-0.0095i$, respectively. On the other hand, at the middle ($k_p = 0.275$ and $k_d = 0.0275$), first and second poles are $+1.3832i$ and $-1.3832i$, respectively. Likewise, close-loop system is stable for proportional gain from 0.0001 to 0.275 and derivative gain from 0.00001 to 0.0275, thus, the proportional gain $k_p = 0.04$ and derivative gain $k_d = 0.004$ will be used.

Then, poles are:

$$\begin{aligned} p_1 &= -0.0146 + 1.4706i, \\ p_2 &= -0.0146 - 1.4706i, \\ p_3 &= -0.0019 + 0.1923i, \\ p_4 &= -0.0019 - 0.1923i, \end{aligned}$$

dominant poles are p_3 and p_4 because they are more closer to 0. Hence, Figure 8 describes step response of close-loop system and time characteristic are:

$$\begin{aligned}w_n &= 0.1923 \frac{\text{rad}}{\text{s}}, \\ \zeta &= 0.0962, \\ \%PO &= 73\%, \\ Ts &= 216 \text{ s}.\end{aligned}$$

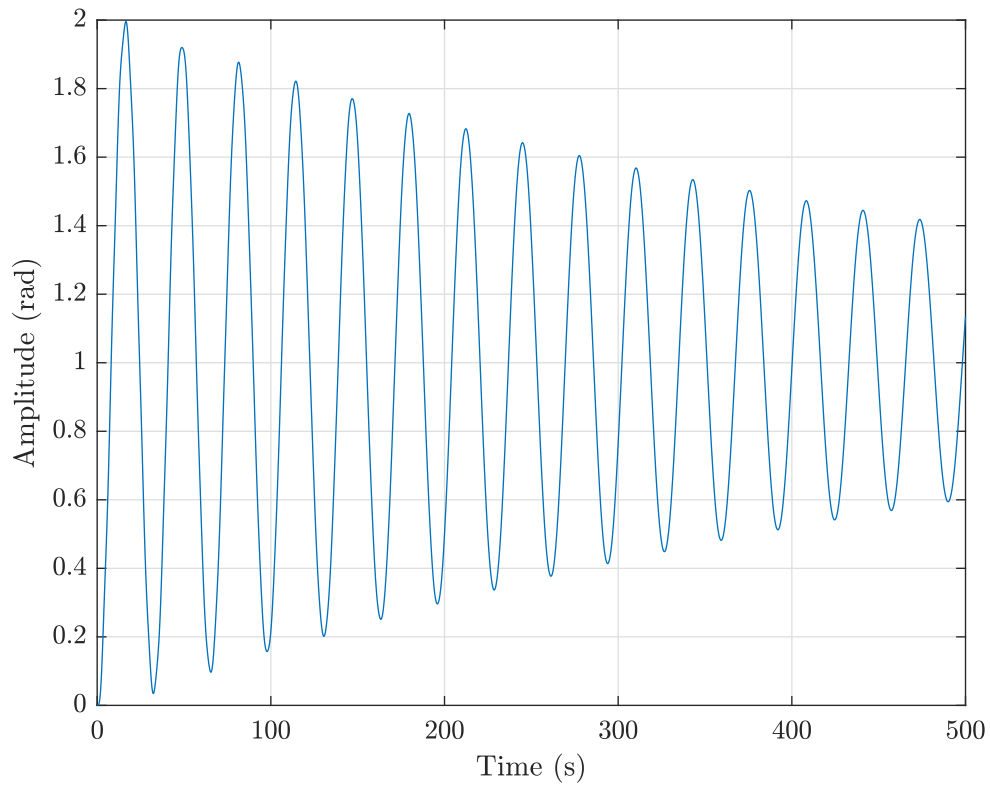


Figure 8: Step response of close-loop system with proportional-derivative control method.

(g) Figure 9 describes bode diagram of Notch filter $N(s) = \frac{s^2+1}{(s+10)^2}$. On one hand, magnitude graph indicates that filter will help to increase gain margin of close-loop system. On the other hand, phase graph indicates that filter will to increase phase margin with a shift of $+180^\circ$.

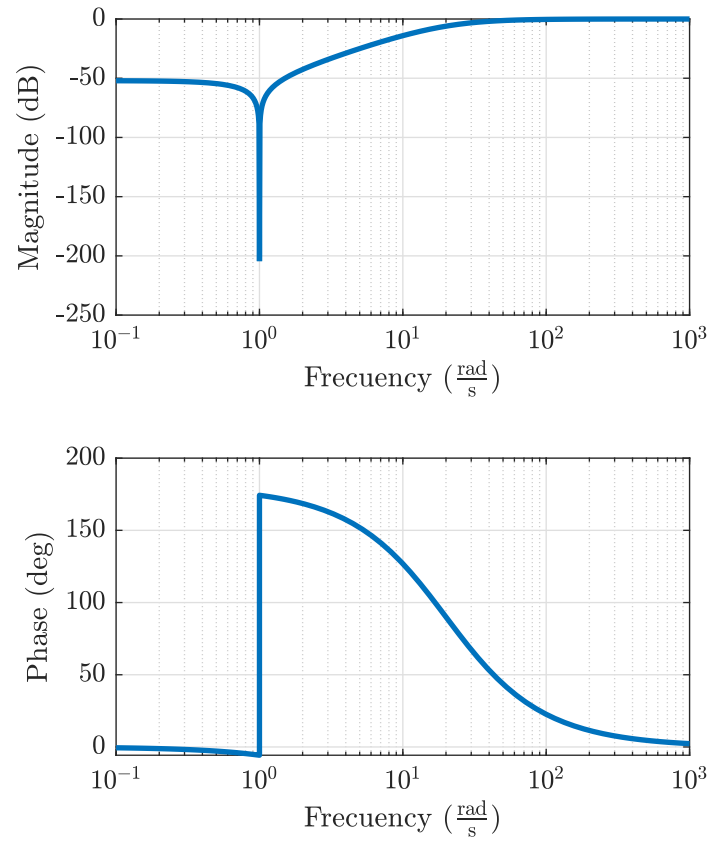


Figure 9: Frequency response of Notch filter.

(h) Figure 10 and 11 describe time and frequency response of close loop system with filter of Notch and proportional-derivative control method. In these figures, time requirements (overshoot $< 15\%$ and settling time < 20) and frequency requirements ($PM > 50^\circ$) are satisfied.

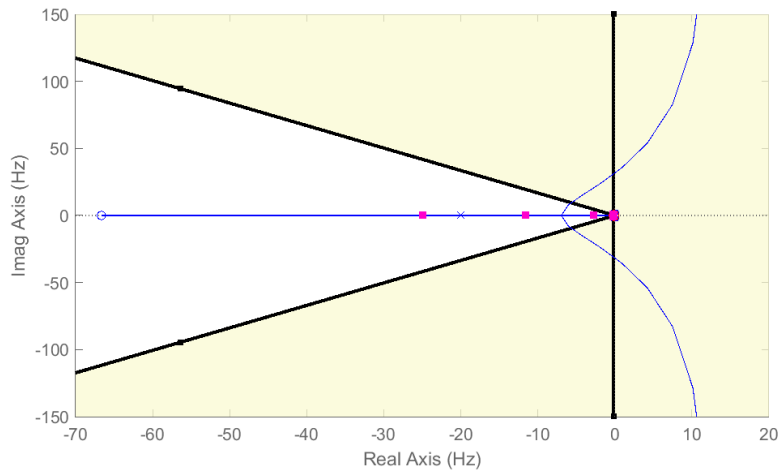
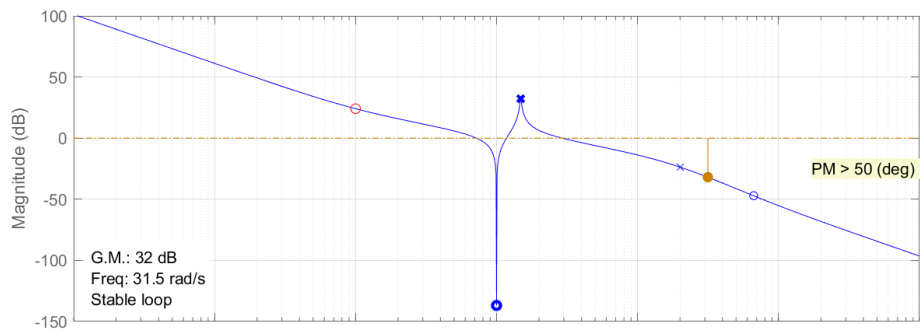
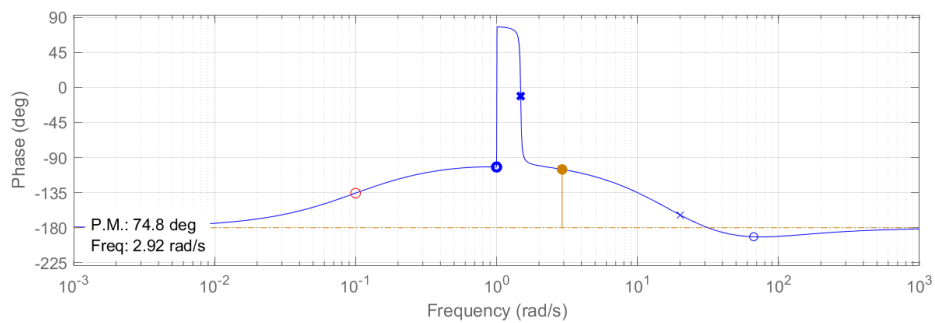


Figure 10: Close-loop system pole location diagram with filter of Notch and proportional-derivative control method.



(a)



(b)

Figure 11: Frequency response of close-loop system with filter of Notch and proportional-derivative control method.

(i) Figure 12 describes step response for six different values of stiffness ($K = 10^{-1}[1, 1.4, 1.8, 2.2, 2.6, 3] \frac{\text{N.m}}{\text{rad}}$) and damping ($D = 10^{-3}[1, 1.8, 2.6, 3.4, 4.2, 5] \frac{\text{N.m.s}}{\text{rad}}$). Hence, system with lower K , D (line blue) have low overshoot and high steady-state error; whereas system with high K , D (line light blue) have high overshoot and low steady-state error.

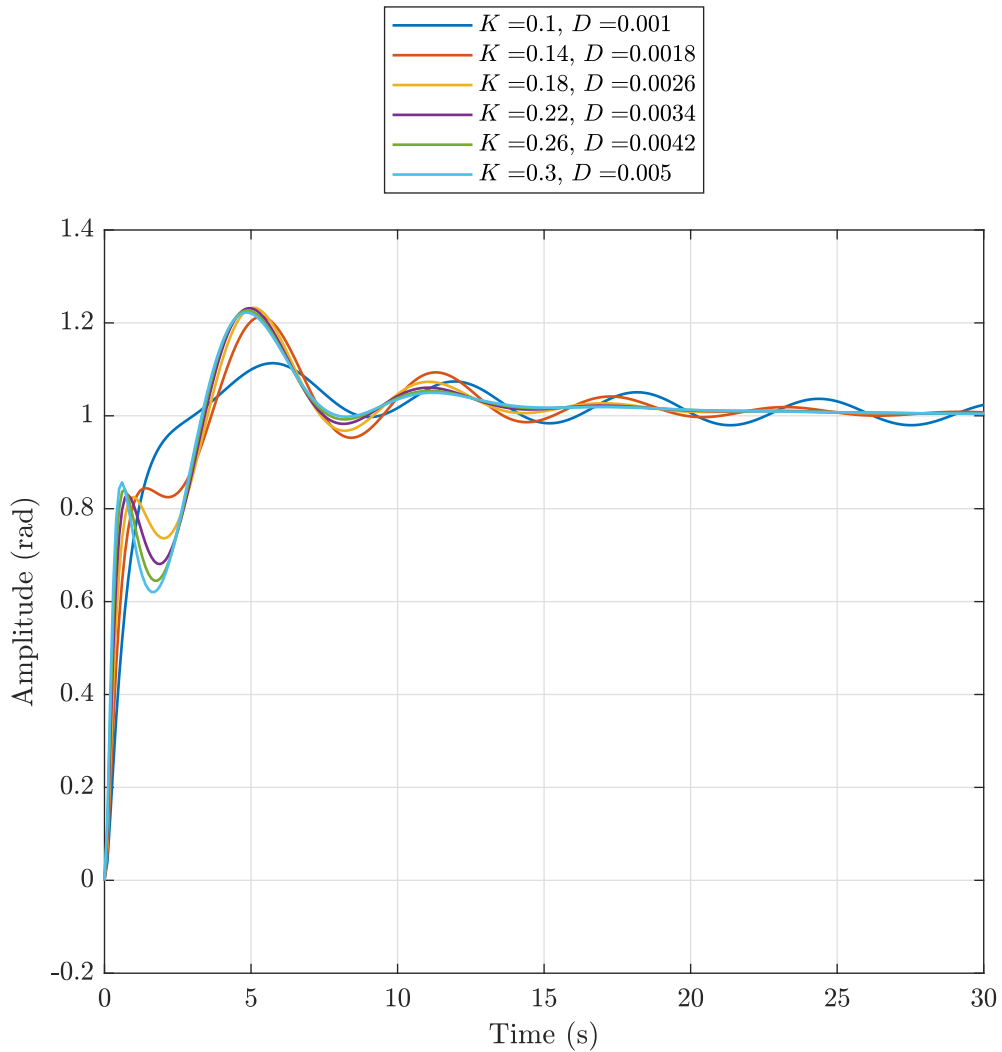


Figure 12: Step response of close-loop system with filter of Notch and proportional-derivative control method for six different values of stiffness (K) and damping (D).